Molecular Cell, Vol. 7, 887–898, April, 2001, Copyright ©2001 by Cell Press

A Block to mRNA Nuclear Export in *S. cerevisiae* Leads to Hyperadenylation of Transcripts that Accumulate at the Site of Transcription

Torben Heick Jensen, Kimberly Patricio, Terri McCarthy, and Michael Rosbash*
Howard Hughes Medical Institute and
Department of Biology
Brandeis University
Waltham, Massachusetts 02454

Summary

Several factors contribute to nuclear mRNA export in *Saccharomyces cerevisiae*, including Mex67p, Mtr2p, Gle1p, Nup159p, Dbp5p, and Rip1p. Strains carrying mutations in these factors show rapid and dramatic nuclear accumulation of poly(A)$^+$ RNA. We have characterized two heat shock mRNAs, *SSA4* and *HSP104*, in these mutant backgrounds; each transcript concentrates in a single intranuclear focus. Evidence suggests that it coincides with the site of transcription. Interestingly, all detectable *SSA4* transcripts have undergone 3′-end formation, indicating that RNAs in the foci are no longer nascent. Poly(A) tails of the transcripts are also dramatically longer in all of these export mutants. Based on all of the data, we suggest that very early mRNA maturation events determine transcript export competence.

Introduction

Exchange of macromolecules between the nucleus and cytoplasm occurs through aqueous holes in the nuclear envelope, the nuclear pore complexes (NPCs). Proteins termed nucleoporins (Nups) assemble to comprise the NPC, which ranges in size from approximately 50 MDa in *S. cerevisiae* to 125 MDa in higher eukaryotes (Feldherr et al., 1984; Stoffler et al., 1999; Rout et al., 2000). A recent exhaustive analysis of *S. cerevisiae* NPCs yielded an upper limit estimate of approximately 30 distinct components. About half of the Nups contain degenerate phenylalanine-glycine (FG) repeats, which are believed to constitute docking sites on the NPC for transport factors (Rout et al., 2000).

Active transport through the NPC is a signal-mediated process (Mattaj and Englmeier, 1998; Nakielny and Dreyfuss, 1999). Nuclear localization signals (NLSs) and nuclear export signals (NESs) direct proteins for nuclear import and export, respectively. Localization signals are generally recognized by transport receptors from the importin-β-like family (importins and exportins), which in *S. cerevisiae* includes 14 members (Wozniak et al., 1998). All transport receptors share an N-terminal domain involved in binding the GTPase Ran and are thought to mediate the directional movement of their cargos through interactions with Ran and FG repeat–containing Nups (Gorlich et al., 1997; Izaurralde et al., 1997).

*To whom correspondence should be addressed (e-mail: rosbash@brandeis.edu).

In yeast, known export substrates include proteins as well as tRNAs, rRNAs, and mRNAs. Signals for nuclear export of RNAs are thought not to reside in the RNA molecule itself but rather in proteins decorating the RNA. An exception is tRNA; the tRNA export receptor exportin-t (higher eukaryotes)/los1p (*S. cerevisiae*) binds directly to both the mature tRNA and RanGTP to form an export-competent trimeric complex (Arts et al., 1998; Kutay et al., 1998; Sarkar and Hopper, 1998). Interestingly, tRNA is the only RNA species in yeast that has been shown to utilize an exportin for nuclear export. It remains unclear whether rRNA and mRNA follow this paradigm for nuclear export by utilizing an export receptor from the importin-β family.

A considerable number of factors have been linked to mRNA export. Most of these were initially identified in *S. cerevisiae* by screening for temperature-sensitive mutants that accumulate poly(A)$^+$ RNA in their nuclei at the restrictive temperature, or through various genetic screens for interactions with Nups or other transport-related factors (Stutz and Rosbash, 1998; Nakielny and Dreyfuss, 1999). Prominent are Mex67p, Mtr2p, Dbp5p/Rat8p, Gle1p, Nup159p/Rat7p, and Nup42p/Rip1p, as conditional mutation or deletion of these proteins results in nuclear accumulation of poly(A)$^+$ RNA within 15 min of a shift to the restrictive temperature (Gorsch et al., 1995; Murphy and Wente, 1996; Santos-Rosa et al., 1998; Snay-Hodge et al., 1998; Tseng et al., 1998; Hurt et al., 2000; this study). Furthermore, all have candidate orthologs that have also been implicated in nuclear export processes in higher eukaryotes (Watkins et al., 1998; Katahira et al., 1999; Schmitt et al., 1999; Strahm et al., 1999). Mex67p shuttles between the nucleus and the cytoplasm, and a Mex67p/Mtr2p complex has been shown to interact with both mRNA as well as components of the NPC and thus might constitute a mobile component of the mRNA export machinery (Segref et al., 1997; Santos-Rosa et al., 1998; Strasser et al., 2000). Dbp5p, an ATP-dependent RNA helicase, also shuttles between the nucleus and the cytoplasm, although with a highly enriched steady-state localization around the nuclear envelope (Snay-Hodge et al., 1998). It physically interacts with Nup159p and Gle1p, suggesting that the contact of Dbp5p to the nuclear envelope might be mediated by these proteins (Snay-Hodge et al., 1998; Strahm et al., 1999; Tseng et al., 1998). Immunoelectron microscopy has localized Nup159p and Gle1p to the cytoplasmic side of the NPC (Rout et al., 2000). The FG repeat–containing protein Rip1p also localizes to the cytoplasmic side of the NPC, although a fraction of Rip1p is detected in the nucleoplasm (Strahm et al., 1999; Rout et al., 2000). *GLE1* mutant alleles are synthetically lethal with a *RIP1* deletion. The C terminus of Rip1p, devoid of all FG repeats, interacts directly with Gle1p and is sufficient to rescue the synthetic lethality of the *GLE1* mutants (Stutz et al., 1997; Strahm et al., 1999). A Rip1p deletion strain exhibits a block to mRNA export only at 42°C, and Rip1p was originally proposed to exercise a role dedicated to the export of heat shock mRNAs (hs-mRNAs; Saavedra et al., 1997). However, recent re-

sults from our laboratory have shown that Rip1p also participates in export of non-hs-mRNAs at 42°C (Vainberg et al., 2000). In addition, other general mRNA export factors are involved in the export of hs-mRNAs at elevated temperatures (Hurt et al., 2000; Vainberg et al., 2000), suggesting that the two mRNA classes are exported via similar pathways.

Interestingly, the Mex67p/Mtr2p complex also connects to Nup159p and Rip1p, as interactions between Mex67p and both Rip1p and Nup159p have been reported (Katahira et al., 1999; Strasser et al., 2000). Thus, mRNA export complexes might pass through a terminal step at the cytoplasmic side of the NPC, defined by the factors Dbp5p, Nup159p, Gle1p, and Rip1p. At this site, mRNP remodeling could take place to facilitate dissociation and recycling of factors with nuclear functions as well as the association of factors with strictly cytoplasmic roles.

Before mRNA can leave the nucleus, appropriate processing events such as capping, splicing, and polyadenylation have to occur. Addition of the poly(A) tail to the nascent transcript takes place after the entire pre-mRNA has been synthesized and cleaved. In *S. cerevisiae*, nuclear cleavage of the pre-mRNA by cleavage factors IA, IB. and II (CFIA, CFIB, and CFII) is directed by signal sequences in the 3′UTR of the nascent transcript (Zhao et al., 1999). Poly(A) tail addition is mediated through the combined action of CFIA, CFIB, polyadenylation factor I (PFI), poly(A) polymerase (PAP), and poly(A) binding protein I (PabI). The polyadenylation reaction deposits a poly(A) tail with a highly defined length, which is organism- and mRNA species-specific. In yeast, newly synthesized poly(A) tails range from ~55–90 nucleotides (nt), whereas in mammals poly(A) tails are ~150–250 nt in length (Brown and Sachs, 1998; Zhao et al., 1999). It is unclear how poly(A) tail length control is achieved in yeast, but it has been suggested to require factors that affect the processivity of PAP or that process the poly(A) tail after poly(A) polymerization (Brown and Sachs, 1998). For example, the poly(A)-specific nuclease (PAN) has been reported to trim newly synthesized poly(A) tails to a species-specific length (Brown and Sachs, 1998). However, it is unknown whether PAN-dependent deadenylation is a nuclear or a cytoplasmic event. Subsequent to proper nuclear processing, polyadenylated mRNAs are then exported to the cytoplasm, translated, and shortened by cytoplasmic nucleases (Zhao et al., 1999).

Evidence exists linking proper 3′-end formation to mRNA export (Eckner et al., 1991). In *S. cerevisiae*, absence of a polyadenylation signal leads to nuclear retention of pol II transcripts (Long et al., 1995). Furthermore, bypassing the cellular cleavage/polyadenylation machinery results in decreased nuclear export of reporter transcripts (Huang and Carmichael, 1996). Thus, it is likely that early steps in mRNA maturation function in part to prepare an mRNA for nuclear export.

In this paper, we investigate the fate of specific transcripts in a variety of *S. cerevisiae* mRNA export mutants. We discover that a block to nuclear export leads to dramatic and rapid effects on polyadenylation and localization of hs mRNAs. Specifically, *SSA4* and *HSP104* transcripts are found to be sequestered in transcription spots within the nucleus. Surprisingly, these mRNAs are processed with poly(A) tails 70–90 nt longer than in a wild-type background. Our results suggest that mRNA export mutant effects take place in part through effects on polyadenylation and/or release of the transcript from the site of transcription.

Results

Absence of Rip1p Results in Hyperadenylation of Heat Shock mRNAs at 42°C

Several papers have previously described the importance of Rip1p for production of heat shock proteins at 42°C (Saavedra et al., 1997; Stutz et al., 1997; Vainberg et al., 2000). In a *RIP1* deletion strain (ΔRIP1), heat shock protein synthesis is eliminated. In situ hybridization experiments with probes directed against bulk poly(A)$^+$ RNA as well as hs-mRNAs showed that this phenotype is due to an mRNA export block (Saavedra et al., 1997; Vainberg et al., 2000). In an attempt to characterize mRNAs retained in the nucleus, we examined the 3′ ends of two hs-mRNAs, *HSP104* and *SSA4*. For this purpose, we employed the PCR- based ligation-mediated poly(A) test assay (LM-PAT) devised by Strickland and colleagues (Salles et al., 1999). This method measures the poly(A) tail length of any transcript by using a transcript-specific primer in the PCR reaction.

HSP104 and *SSA4* transcription was induced by shifting the growth temperature from 25°C to 42°C. These two transcripts are undetectable at 25°C by primer extension analysis (Stutz et al., 1997 and data not shown), so the temperature shift provides a tight on/off system of transcriptional induction. To analyze newly synthesized transcripts, cells were harvested at different time points starting as early as 30 s after induction. In a wild-type W303 strain, *HSP104* and *SSA4* transcripts appeared immediately, with a maximal poly(A) tail length of approximately 80 nt (Figures 1A and 1B, lanes 2 and 3). This length is comparable to the average length of poly(A) tails of other yeast mRNAs (Zhao et al., 1999). After longer incubation times at 42°C, the average distribution shifted toward a population with shorter poly(A) tails (Figures 1A and 1B, lanes 4–7). This evolution is expected since the RNAs are being exported to the cytoplasm and gradually deadenylated and degraded during translation. Surprisingly, the average poly(A) tail length of both transcripts was much greater in the ΔRIP1 strain. In this case, they appeared with a maximal poly(A) tail length of ~160 nt, with an average distribution clearly in favor of the maximal length. Within the time span of the experiment, this distribution did not change markedly (Figures 1A and 1B, lanes 9–15). Since the PCR part of the LM-PAT method favors amplification of the smaller fragments (data not shown), a conservative estimate is that at least 95% of total polyadenylated *HSP104* and *SSA4* transcripts appear with long poly(A) tails when export of these transcripts is inhibited in the ΔRIP1 strain.

We also performed oligo(dT)/RNaseH-Northern analysis on *SSA4* mRNA from the W303 and ΔRIP1 strains. Hybridization was carried out with probes against the 3′UTR of the *SSA4* transcript. To evaluate the size contribution of the poly(A) tails, total RNA samples were incubated with or without oligo(dT) during the RNaseH treat-

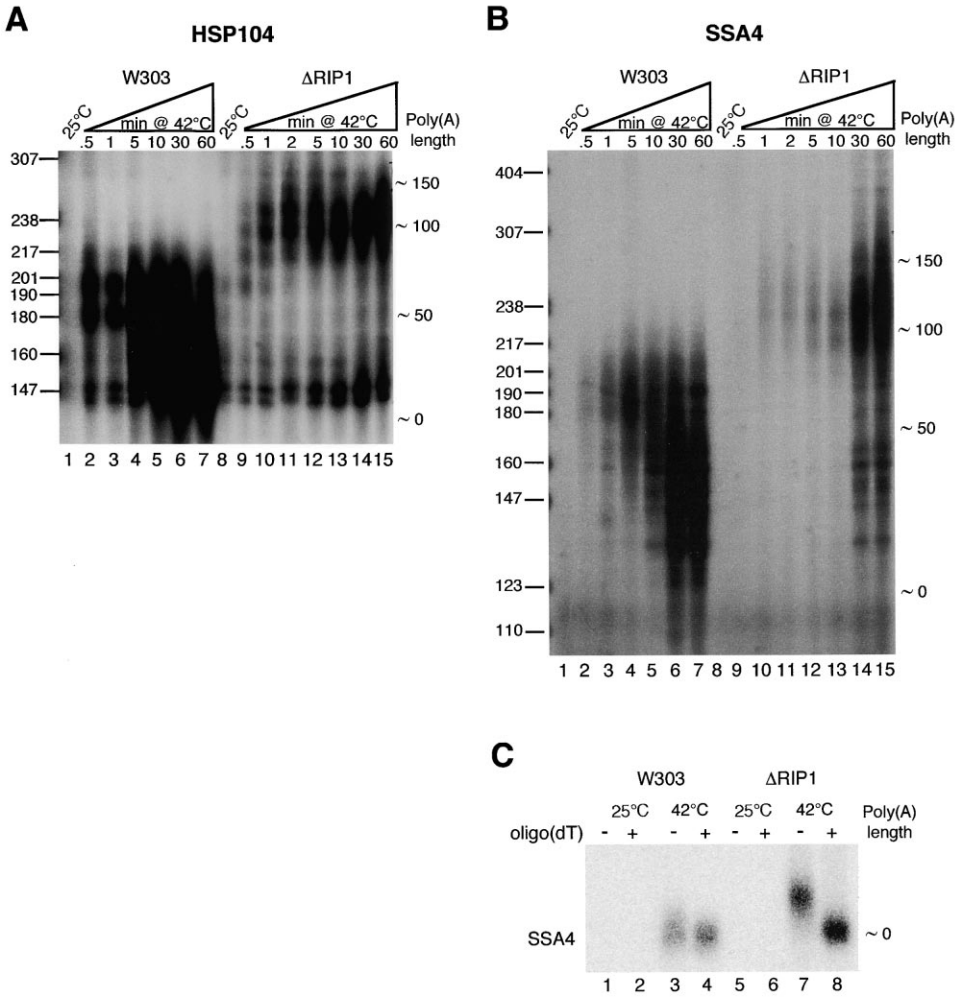

Figure 1. Analysis of *HSP104* and *SSA4* mRNA Poly(A) Tail Lengths upon Transcriptional Induction in Wild-Type W303 and Rip1p Deletion Strains

(A) Total RNA was isolated from cultures of W303 or ΔRIP1 strains incubated at 25°C or temperature shifted to 42°C for various times. RNA from individual samples were analyzed by the LM-PAT assay using *HSP104*-specific primer (iv93). The lowest migrating product corresponds to a small amount of priming of the oligo(dT)-anchor primer from the 5′ end of the poly(A) tail. Estimated sizes of poly(A) tails are given to the right of the gel, and migration of radioactive DNA size markers is indicated to the left.

(B) LM-PAT analysis of samples described in (A) with an *SSA4*-specific primer (kp19).

(C) Oligo(dT)/RNaseH-Northern analysis for *SSA4* mRNA isolated from W303 and ΔRIP1 strains grown at either 25°C or temperature shifted to 42°C for 60 min. Hybridization was done with 5′-end labeled 3′UTR *SSA4* antisense probes kd199 and kd200. To increase resolution, *SSA4* mRNA was internally cleaved with an *SSA4* antisense oligo and RNaseH. RNaseH digestion was carried out either in the absence (−) or presence (+) of an oligo $(dT)_{18}$ as indicated. Estimated sizes of poly(A) tails are given to the right of the image.

ment. Consistent with the data obtained from LM-PAT analysis, *SSA4* transcripts migrate more slowly when RNA is isolated from the ΔRIP1 strain as compared to W303 at 42°C (Figure 1C, compare lanes 3 and 7). This mobility change is due to lengthening of the *SSA4* poly(A) tail, as oligo(dT)/RNaseH-directed poly(A) tail removal results in a species that now migrates comparably to oligo(dT)/RNaseH-treated *SSA4* mRNA from a W303 strain (Figure 1C, compare lanes 4 and 8).

Two important points can be made from the oligo(dT)/RNaseH-Northern analysis. First, the lengthening of the *SSA4* LM-PAT product at 42°C in the ΔRIP1 strain is due to a longer poly(A) tail rather than utilization of an alternative downstream polyadenylation/cleavage site in the *SSA4* 3′UTR. This conclusion is strengthened by sequencing of *SSA4* RT–PCR products from ΔRIP1 and W303 strains at 42°C; there is no difference in the poly(A) addition site (data not shown). Second, the oligo(dT)/RNaseH-Northern analysis shows that nearly the entire population of *SSA4* mRNA in the ΔRIP1 strain is hyperadenylated at 42°C . This is important, as a limitation of the LM-PAT assay is that it only detects polyadenylated species.

HSP104 and *SSA4* mRNAs Localize to an Intranuclear Dot in the Absence of Rip1p

We have previously observed that the nuclear accumulation of *SSA4* mRNA in ΔRIP1 at 42°C is morphologically distinct from that of bulk poly(A)$^+$ RNA (Vainberg et al., 2000). To examine the generality of this phenomenon,

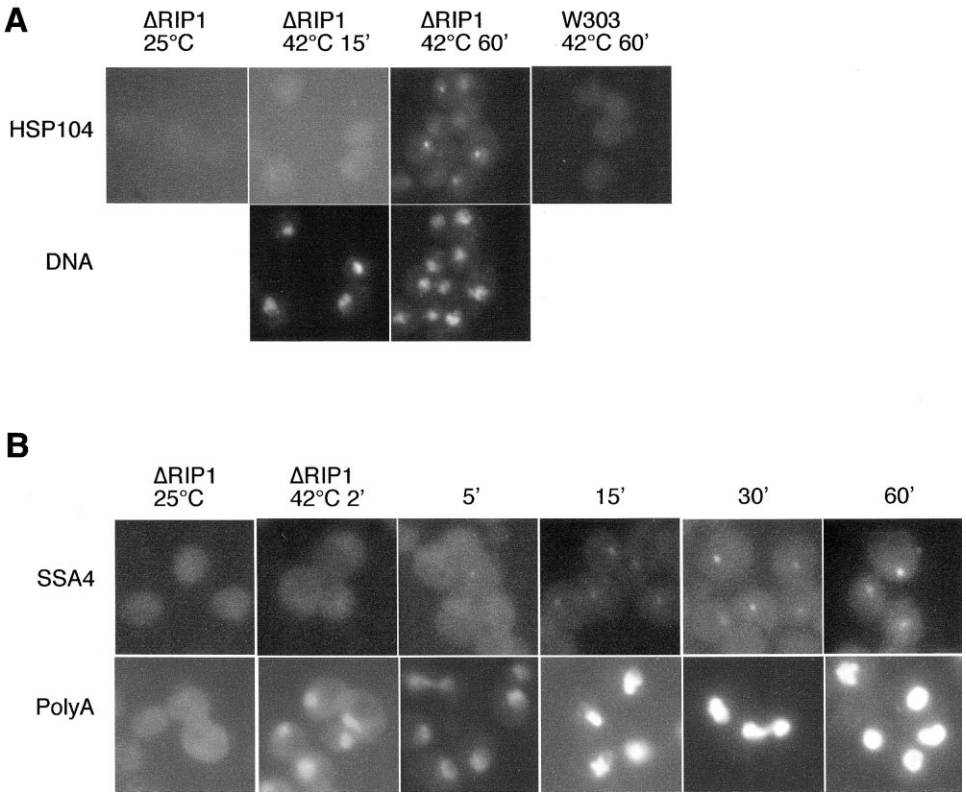

Figure 2. *HSP104* and *SSA4* mRNAs Localize to Intranuclear Foci in ΔRIP1 at the Restrictive Temperature

(A) *HSP104* mRNA-FISH analysis on cultures grown at 25°C (ΔRIP1) or temperature shifted to 42°C for 15 min (ΔRIP1) or 60 min (ΔRIP1 and W303), as indicated. *HSP104* mRNA localization was visualized using Cy3-labeled oligonucleotides (thj203, thj204, thj205, and thj206). DAPI (4′,6′-diamidino-2-phenylindole) staining for the ΔRIP1 strain at 42°C is shown in the lower panel.

(B) *SSA4* mRNA- and poly(A)$^+$ RNA-FISH analysis in ΔRIP1 at 25°C and after temperature shift to 42°C for various times as indicated. *SSA4* mRNA was visualized using Cy3-labeled oligonuceotides (kd199 and kd200), and poly(A)$^+$ RNA was visualized with Cy3-labeled oligo(dT)$_{70}$. DAPI staining was used to verify the nuclear localization of the *SSA4* and poly(A)$^+$ RNA signals (data not shown).

we analyzed the localization of *HSP104* mRNA under similar conditions by fluorescent in situ hybridization (FISH). After a 15 min shift of the ΔRIP1 strain to 42°C, localized nuclear foci were detected that increased in intensity with longer incubation (Figure 2A). No *HSP104* signal was detectable in W303 at 42°C or in ΔRIP1 at 25°C, and fluorescently labeled sense oligonucleotides did not yield a signal over background when employed in the RNA-FISH procedure (data not shown). We conclude that the signal originates from probes annealing to the *HSP104* mRNA, as opposed to the *HSP104* gene. The accumulation of *HSP104* mRNA in a "nuclear dot" is, therefore, comparable to what was observed for *SSA4* mRNA (Vainberg et al., 2000 and Figure 2B).

We next examined the kinetics by which the *SSA4* nuclear dot signal appears after a shift to 42°C in the ΔRIP1 strain. The signal is detectable in some cells as early as 5 min after the temperature shift, becomes visible in all cells after 15 min, and is very prominent after 30 and 60 min (Figure 2B). Interestingly, the *SSA4* FISH signal intensity time course correlates well with the appearance of hyperadenylated *SSA4* mRNA in ΔRIP1 as determined by LM-PAT (Figure 1B, lanes 9–15). The *SSA4* FISH analysis was carried out with the same probes used in the RNaseH/oligo(dT) Northern analysis. These probes detected exclusively *SSA4* mRNA with extended poly(A) tails (Figure 1C). We therefore conclude that the in situ signal originates from hyperadenylated *SSA4* mRNAs. Thus, most if not all of the *SSA4* mRNAs in the nuclear dot in ΔRIP1 are cleaved and polyadenylated.

Fixed ΔRIP1 cells were also probed with a fluorescent oligo(dT) probe to visualize total poly(A)$^+$ RNA. Nuclear accumulation of poly(A)$^+$ RNA is extremely fast under these experimental conditions: a robust nuclear signal is detectable as early as 2 min after the temperature shift (Figure 2B, lower panel). The strong poly(A)$^+$ signal in ΔRIP1 might in part reflect hs-mRNAs, as previously discussed (Vainberg et al., 2000).

The Nuclear *SSA4* mRNA Signal Is at the Site of Transcription

To address further the nature of the *SSA4* mRNA dot, we performed FISH in a diploid strain deleted for both copies of the *RIP1* gene. In this strain, the *SSA4*-specific probe gives rise to two nuclear dots (Figure 3, middle panel). The *SSA4* "double dots" were prominent and present in at least 90% of inspected cells (data not shown). We interpret these data to show that the nuclear *SSA4* mRNA signal is at or very near the site of *SSA4* transcription. This idea is substantiated by the fact that the *SSA4* mRNA FISH signal is much more disperse in

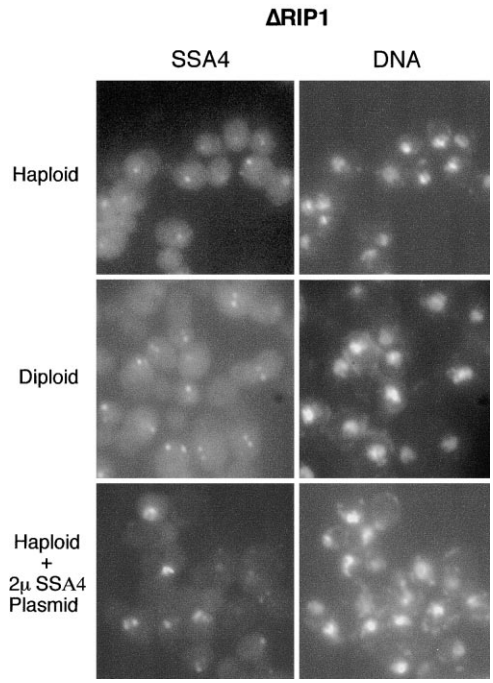

Figure 3. *SSA4* mRNA-FISH Analysis of Haploid, Diploid, and 2 μ High Copy SSA4-Plasmid-Containing Haploid ΔRIP1 Strains

Cultures were temperature shifted to 42°C for 30 min, and *SSA4* mRNA and DNA staining was performed as described in Figure 2. Upon inspection of larger fields of view, one and two intranuclear *SSA4* mRNA dots were observed in over 90% of the ΔRIP1 haploid and diploid cells, respectively.

a haploid ΔRIP1 strain transformed with a multicopy plasmid containing the *SSA4* gene, consistent with the presence of many transcription sites (Figure 3, lower panel). With a low copy number plasmid, one to four dots were observed, also consistent with a transcription spot interpretation (data not shown).

Expression of a Truncated Rip1p Protein Devoid of Its FG Repeats Relieves *SSA4* mRNA Nuclear Dot Formation and Results in Poly(A) Tail Shortening

We previously reported that the FG repeat region of Rip1p is inessential for hs-mRNA export, since expression of the unique C-terminal 66 amino acids of Rip1p restores heat shock protein synthesis in a ΔRIP1 background (Stutz et al., 1997). We therefore examined the effect of this Rip1p C-terminal fragment (RIP1-0FG) on the *SSA4* mRNA nuclear dot and on the long poly(A) tail phenotypes of the ΔRIP1 strain. In this analysis, two other Rip1p expression constructs were also employed. The constructs RIP1-HI and RIP1-LO constitute plasmid versions of two different genomic *RIP1* fragments that express high and low levels of Rip1p, respectively (Stutz et al., 1997).

SSA4 mRNA FISH analysis revealed that all three Rip1p constructs rescued the nuclear dot accumulation phenotype of the ΔRIP1 strain at 42°C (Figure 4A, for RIP-HI and RIP1-LO compare rows 1–3 and for RIP1-0FG compare rows 4 and 5). The efficiency of RIP1-LO was less robust, as a low-intensity nuclear dot was observed in a small fraction of these cells (data not shown). Examination of the *SSA4* mRNA 3′ ends by LM-PAT showed that all three Rip1p-expressing constructs restored *SSA4* poly(A) tail length to that observed in wild type (Figure 4B and data not shown).

Finally, we analyzed the ability of the three Rip1p constructs to rescue heat shock protein synthesis at 42°C in the ΔRIP1 strain. As previously noted, high amounts of Rip1p (from RIP1-HI) and the C terminus of Rip1p (from RIP1-0FG) restore heat shock protein synthesis at 42°C (Figure 4C, lanes 5 and 6 and lanes 14 and 15). Low expression of Rip1p (RIP1-LO) results in a more modest induction of heat shock proteins (Figure 4C, lanes 8 and 9). This intermediate phenotype is consistent with the intermediate rescue by RIP1-LO in the *SSA4* mRNA FISH experiment. In a previous report, low expression of Rip1p did not result in detectable heat shock protein synthesis (Stutz et al., 1997). The reason for this discrepancy is not clear, although it has been noted that culture density affects the efficiency of heat shock protein synthesis. For that reason, the assays described here were all done under similar experimental conditions.

In conclusion, there is a good correlation between the ability of the different Rip1p-expressing plasmids to rescue the *SSA4* mRNA nuclear dot accumulation, induce shortening of the *SSA4* mRNA poly(A) tail, and restore heat shock protein synthesis. This correlation suggests that the lack of heat shock protein synthesis at 42°C in the ΔRIP1 strain is caused, at least in part, by the inability of hs-mRNAs to leave their sites of transcription.

Several mRNA Export Mutants Accumulate Hyperadenylated *SSA4* mRNA in Nuclear Dots

The C-terminal portion of Rip1p has been previously reported to interact directly with Gle1p (Strahm et al., 1999), an interaction that probably takes place on the cytoplasmic face of the NPC. This suggests that the two intranuclear phenotypes of *SSA4* mRNA are not directly due to a lack of Rip1p in the mRNP formed during or shortly after transcription. We therefore tested the generality of the nuclear dot and hyperadenylation phenotypes by assaying other temperature-sensitive mutants with known defects in mRNA export. When mRNA export mutants *mex67-5*, *rat7-1*, and *rat8-2* were shifted to 42°C and analyzed by FISH, an identical intranuclear *SSA4* dot was readily visible (Figure 5A). The *SSA4* mRNA was also analyzed by the LM-PAT assay, and all three strains contained hyperadenylated *SSA4* mRNA after incubation at 42°C for either 15 or 60 min (Figure 5B). Some tail lengthening was also observed when the cultures were shifted to 37°C (most prominent for *mex67-5*), but both nuclear dot formation and poly(A) tail lengthening were generally more robust at 42°C (Figures 5A and 5B and data not shown). This might reflect a more rapid and robust induction of the mutant phenotype at higher temperatures, or it might be due to physiological differences between the two temperatures. Our results show that nuclear dot accumulation and hyperadenylation of *SSA4* mRNA are a consequence of a general block to nuclear mRNA export.

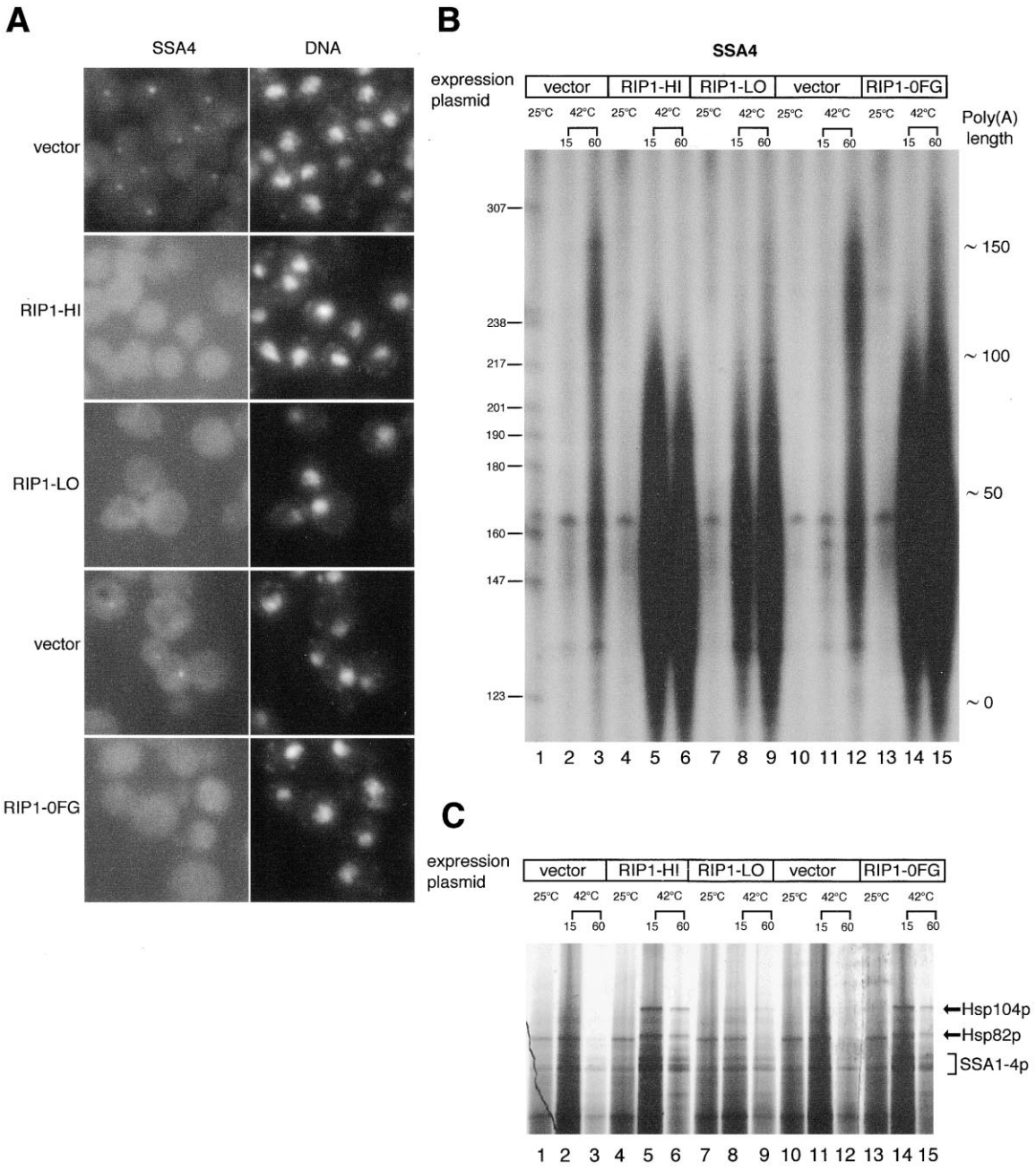

Figure 4. Expression of the Unique C Terminus of Rip1p Rescues the *SSA4*-mRNA-Related Phenotypes in ΔRIP1

(A) *SSA4* mRNA-FISH analysis of the ΔRIP1 strain transformed with plasmids either expressing high amounts of Rip1p (RIP1-HI), low amounts of Rip1p (RIP1-LO), or the unique C terminus of Rip1p (RIP1-0FG) and the corresponding vector controls. Transformed strains were grown at 42°C for 60 min prior to fixation and *SSA4* mRNA-FISH analysis.

(B) LM-PAT analysis of *SSA4* mRNA isolated from the transformed strains described in (A). Cells were harvested after growth at 25°C or after a temperature shift to 42°C for 15 or 60 min. LM-PAT analysis was performed using primer kp19. Estimated sizes of poly(A) tails are given on the right, and migration of a radioactive DNA size marker is given on the left.

(C) Analysis of heat shock protein synthesis in the indicated strains. Cultures were grown as in (B) and subsequently labeled with [^{35}S]methionine at the indicated temperatures. Samples were analyzed by SDS–PAGE and autoradiographed. The positions of heat shock proteins Hsp104p, Hsp82p, and Hsp70ps (Ssa1p, Ssa2p, Ssa3p, and Ssa4p) are indicated.

A General Poly(A) Tail Lengthening in mRNA Export Mutants

HSP104 and *SSA4* are rapidly and robustly induced by a heat shock. It was possible that these heat shock genes are exceptional and that a strong transcriptional response is required for the observed defects in 3′-end formation. We therefore examined the 3′-end status of endogenous *PGK1* mRNA in various mRNA export mutants.

At steady state, a high fraction of mRNA is cyto-

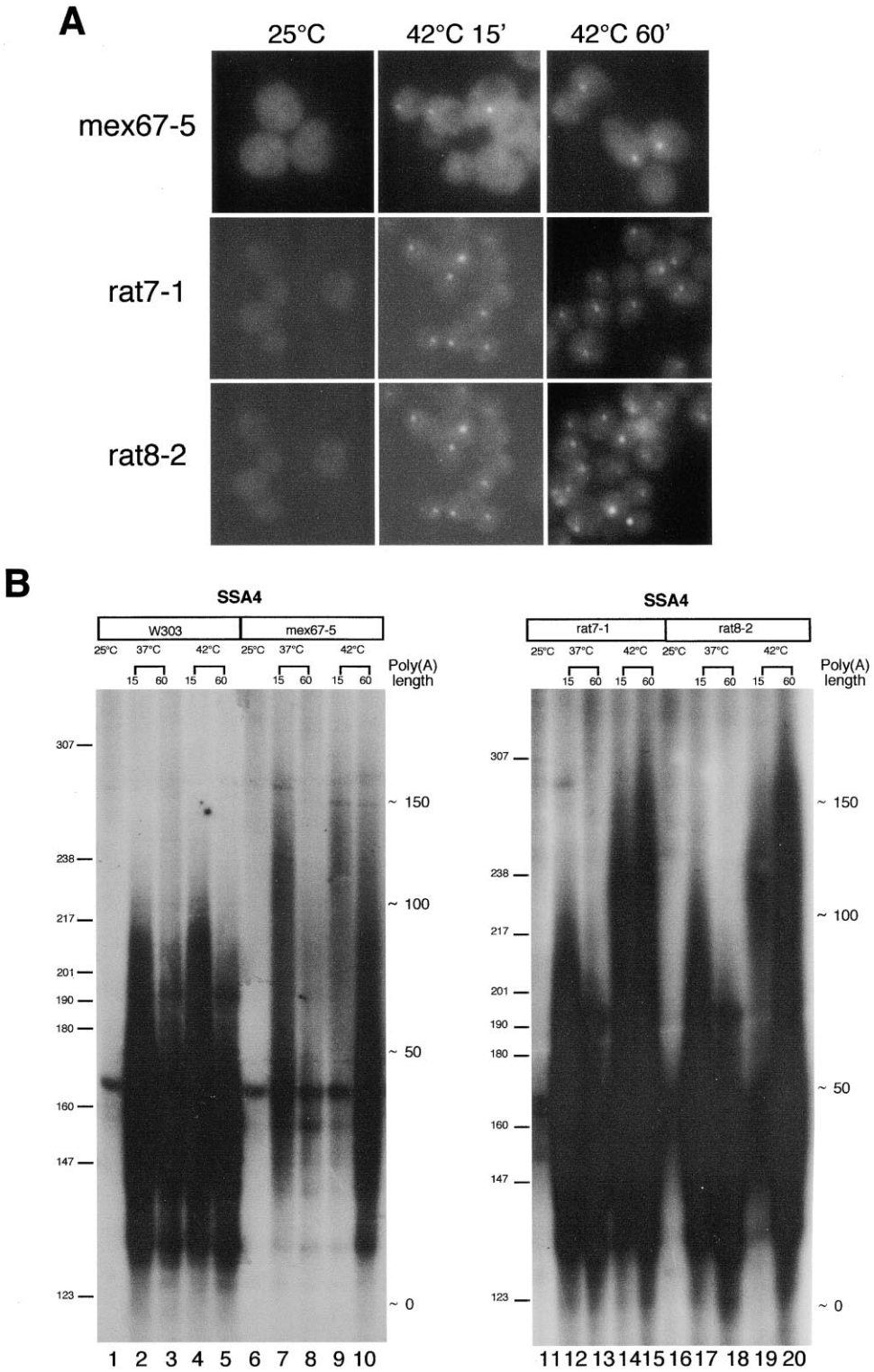

Figure 5. Nuclear Dot Formation and Hyperadenylation of *SSA4* mRNA in Other mRNA Export Mutants

(A) *SSA4* mRNA-FISH analysis in mutant strains *mex67-5*, *rat7-1*, and *rat8-2*. Cells were fixed after growth at 25°C or after temperature shift to 42°C for 15 or 60 min and analyzed by RNA-FISH using Cy3-labeled *SSA4* mRNA–specific probes kd199 and kd200. The intranuclear localization of the *SSA4* mRNA signal was confirmed by DAPI staining (data not shown).

(B) LM-PAT analysis of *SSA4* mRNA isolated from wild-type W303, *mex67-5*, *rat7-1*, and *rat8-2* strains using primer kp19. Cells were harvested after growth at 25°C or after temperature shift to either 37°C or 42°C for 15 or 60 min. Estimated sizes of poly(A) tails are given to the right, and migration of a DNA size marker is given on the left.

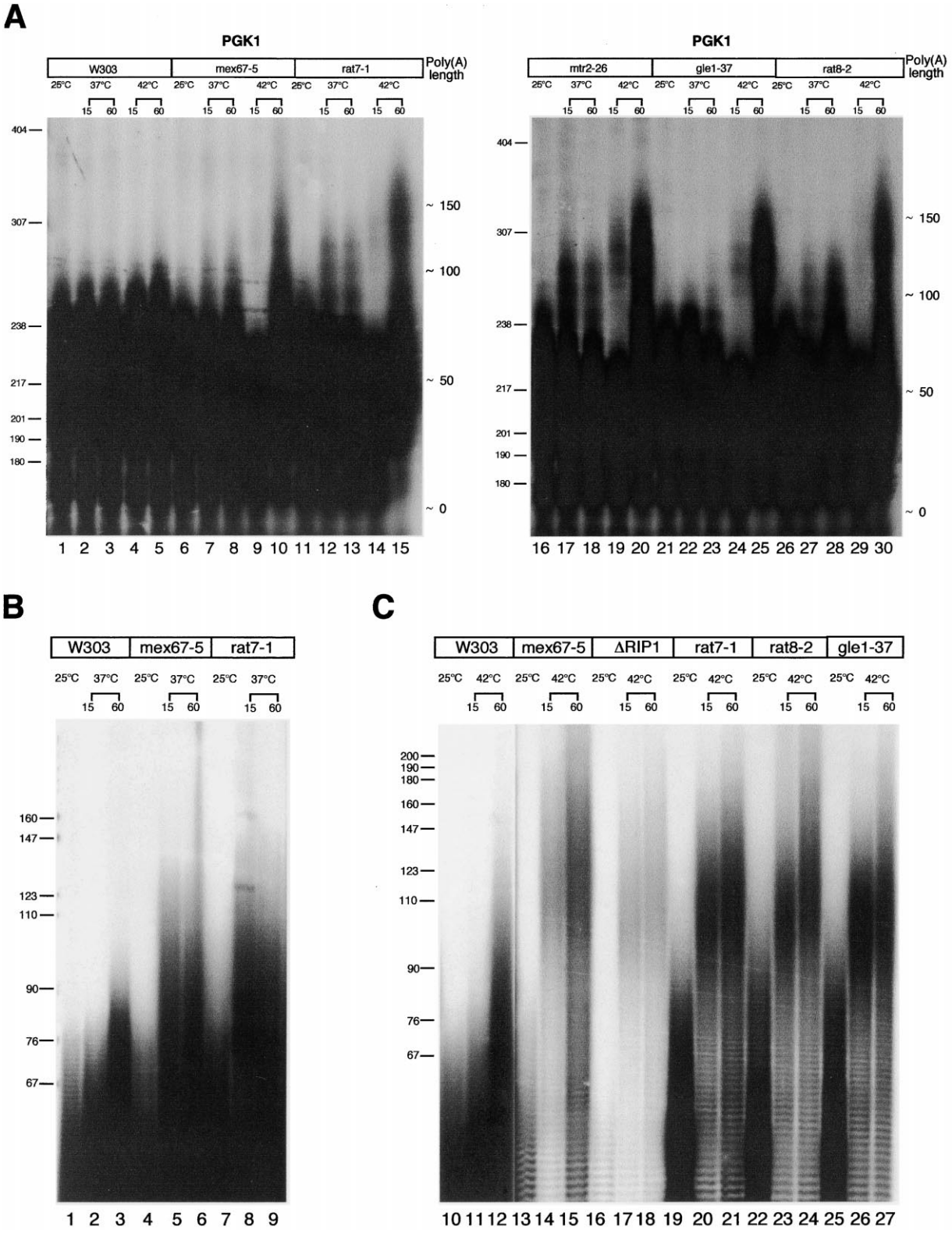

Figure 6. General Hyperadenylation of Transcripts in mRNA Export Mutants

(A) LM-PAT analysis of *PGK1* mRNA isolated from wild-type W303, *mex67-5*, *rat7-1*, *mtr2-26*, *gle1-37*, and *rat8-2* strains as indicated. Cultures were grown as described in Figure 5B. LM-PAT analysis was performed using the *PGK1*-specific primer thj187 (see supplemental Table 2 at www.molecule.org/cgi/content/full/7/4/887/DC1).

(B) Bulk poly(A) tail length determination of RNA isolated from W303, *mex67-5*, and *rat7-1* strains grown at 25°C or temperature shifted to

plasmic. Therefore, a requirement for a specific nuclear mRNA to be detected in the LM-PAT assay is that its transcription is ongoing. Initial attempts to assay the short-lived *TCM1*, *RPS5*, and *URA5* transcripts resulted in a loss of signal at 42°C, presumably due to transcriptional shutdown and/or changes in mRNA turnover rates (data not shown). In contrast, the abundance of *PGK1* mRNA does not change dramatically after a 39°C heat shock (Roth et al., 1998), suggesting that *PGK1* transcription continues at elevated temperatures.

When assayed by LM-PAT, *PGK1* RNA acquired longer poly(A) tails at restrictive temperatures in mRNA export mutants *mex67-5*, *rat7-1*, *mtr2-26*, *gle1-37*, and *rat8-2* (Figure 6A). As observed for *SSA4* and *HSP104* transcripts, the 3′-end lengthening of *PGK1* mRNA was exacerbated after a shift to 42°C as compared to 37°C (Figure 6A, compare, for example, lanes 12 and 13 to lanes 14 and 15). This observation indicates that the hyperadenylation phenotype is a general phenomenon and not restricted to hs-mRNAs.

To further determine if the poly(A) tail lengthening is a general phenomenon, we examined the general length distribution of poly(A) tails in mRNA export mutants. This was done by ^{32}pCp 3′-end labeling of total RNA followed by incubation with RNaseA and T1, which leaves only oligo(A) and poly(A) stretches intact.

RNA isolated from the wild-type W303 strain experienced a tail lengthening of approximately 10–15 nt after incubation at 37°C for 60 min (Figure 6B, compare lanes 1 and 3). However, in *mex67-5* and *rat7-1* strains shifted to 37°C, poly(A) tails were 45–50 nt longer than those observed at 25°C (Figure 6B, compare lanes 5 and 6 and 8 and 9 to lanes 4 and 7). A temperature shift to 42°C enhanced this phenotype, as poly(A) tail lengthening proceeded to 90–100 nts longer than at the permissive temperature (Figure 6C). These observations indicate that hyperadenylation is a general response to an mRNA export block. Hs-mRNA could still constitute a substantial fraction of this more general response.

GAL1 mRNA Forms a Nuclear Dot in the *rat7-1* Strain

To investigate the localization of a non-hs-mRNA under export mutant conditions, endogenous *GAL1* transcripts were analyzed by the RNA-FISH protocol in the *rat7-1* strain (probe sequences were kindly provided by P. Chartrand). *GAL1* transcription was induced after a 15 min preincubation of *rat7-1* at 37°C. In the *rat7-1* mutant, *GAL1* mRNA forms nuclear dots similar to those seen for *Hsp104* and *SSA4* transcripts (Figure 7, middle row). When galactose was not added to the culture medium or when the cells were grown in 2% glucose, the nuclear signal was absent (Figure 7, upper and lower rows, respectively). This result shows that a non-hs-mRNA is also sequestered in a nuclear dot when mRNA export is inhibited and, thus, suggests some generality of this phenomenon.

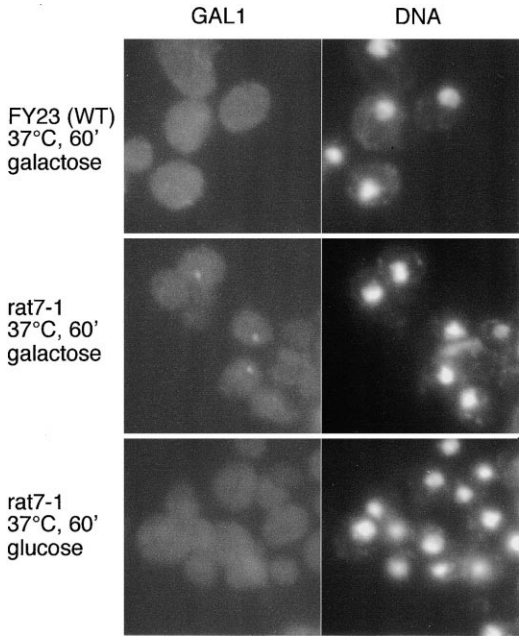

Figure 7. *GAL1* mRNA Localizes to an Intranuclear Dot in rat7-1 at the Restrictive Temperature

GAL1 mRNA-FISH analysis in the *rat7-1* strain or in the corresponding wild-type FY23 strain as indicated. Cells were grown in neutral carbohydrate medium at 25°C. After a temperature shift to 37°C for 15 min, *GAL1* transcription was induced by addition of galactose to 2%, whereafter incubation at 37°C was continued for 60 min. As a control, the *rat7-1* strain was grown in glucose-repressing *GAL1* gene expression. Cells were fixed and analyzed by RNA-FISH using Cy3-labeled *GAL1* mRNA-specific probes (thj290, thj291, thj292, thj293, thj294, and thj295). DAPI staining of cells is also shown.

Discussion

In this study, we have characterized the 3′-end status and subcellular localization of specific mRNAs under conditions that block mRNA export. We have used a range of conditional yeast mutants, all of which have been previously shown to have rapid and dramatic mRNA export phenotypes at the restrictive temperature. We find two general phenotypes associated with the retained mRNAs: (1) they have extended poly(A) tails, and (2) the fluorescent signal detected by transcript-specific RNA-FISH is localized to a well-defined intranuclear focus.

The poly(A) tail lengthening phenotypes are extremely rapid and dramatic when compared to the effects previously observed in mRNA transport mutants (Zhao et al., 1999 and references therein). For example, mutant alleles of the RanGTPase system, *rna1-1* and *prp20-1*, accumulate bulk poly(A)$^+$ RNA in nuclei with poly(A) tails ~15–20 nt longer than usual (Forrester et al., 1992). Moreover, a comparably modest poly(A) tail lengthening

37°C for 15 or 60 min. Total RNA was 3′-end labeled with ^{32}pCp by T4 RNA ligase and digested with RnaseA/T1, which leaves only oligo(A) and poly(A) stretches uncleaved. Migration of a DNA marker is indicated.
(C) Tail length determination of RNA isolated from W303, *mex67-5*, ΔRIP1, *rat7-1*, *rat8-2*, and *gle1-37* strains grown at 25°C or temperature shifted to 42°C for 15 or 60 min.

is observed in yeast strains harboring mutations in other genes with a less defined role in mRNA export (Zhao et al., 1999). Poly(A) tails are trimmed in the cytoplasm, and a lack of nuclear export would leave the transcripts with slightly longer 3′ ends (Forrester et al., 1992).

It is not apparent why some general mRNA export mutants contain dramatically hyperadenylated transcripts, whereas others have more modest effects on 3′-end formation. In these experiments, we have only focused on conditional mutants with rapid and robust mRNA export defects. It is possible that the polyadenylation phenotypes are more severe as a function of the strength of the nuclear mRNA export block. Alternatively, different poly(A) tail lengthening phenotypes could be induced through defects in different cellular events. A related question is whether the presence of hyperadenylated transcripts in the cell reflects a normal process. For example, a nuclear export block might trap a hyperadenylated intermediate due to a defect in a nuclear trimming event. However, we detect no hyperadenylation in a wild-type strain even at very short times after induction (Figures 1A and 1B). Thus, if a hyperadenylated species is present at some point in the mRNA life cycle, it would have to be extremely short lived.

We believe that the intranuclear *SSA4* and *HSP104* mRNA FISH signals coincide with the sites of transcription. The *SSA4* mRNA-FISH analysis revealed two intranuclear dots in a ΔRIP1 diploid strain. If the *SSA4* transcripts were localized to a nuclear substructure unrelated to the *SSA4* gene locus, it would be unlikely that such a structure would double with a doubling of the chromosome number. Furthermore, recent data using a stably transfected murine erythroleukemia cell system revealed that intranuclear foci of the human β-globin mRNA colocalized with the template gene locus (Custodio et al., 1999). In this system, the accumulated transcripts were released by treatment with a transcriptional inhibitor. The authors found no evidence for transcript accumulation at other nuclear locations and suggested that transcripts rapidly diffuse in all directions after release from RNA polymerase II.

How global are the observed phenotypes? We show here that *PGK1* mRNA, which does not undergo massive transcriptional induction under the same experimental conditions, is also hyperadenylated in these mutants. Furthermore, bulk poly(A) tails are lengthened dramatically, indicating a rather general problem with poly(A) tail length control. Endogenous *PGK1* mRNA was recently localized to nuclei by RNA-FISH in the *mex67-5* mutant under restrictive conditions (Hurt et al., 2000). Although granular in appearance, the *PGK1* mRNA signal did not appear discrete, as we observe for *SSA4* and *HSP104* mRNAs, indicating that the *PGK1* transcripts might be more distributed in nuclear space. We have been unable to detect a reproducible *PGK1* mRNA signal under our experimental conditions (data not shown). We therefore performed RNA-FISH on endogenous *GAL1* mRNA and observed a dot-like signal when transcription was induced by galactose addition. Although this observation shows that nuclear sequestration is not restricted to hs-mRNAs, it does not exclude an important role of potent transcriptional induction. Clearly, more transcripts will have to be surveyed.

Our results strongly suggest that hyperadenylation and formation of discrete nuclear foci are functionally linked. The signal strength of hyperadenylated *SSA4* mRNA detected by LM-PAT correlates well with the *SSA4* mRNA-FISH signal intensity at comparable time points (Figures 1B and 2B). Furthermore, overexpression of the unique C terminus of Rip1p rescues both transcript sequestration and hyperadenylation. However, there is some evidence that extreme hyperadenylation might not be required to stall transcripts at transcription sites. For example, we observe more subtle effects on the poly(A) tail length of *SSA4* transcripts at 37°C, yet they are sequestered in transcription spots (Figure 5 and data not shown). In addition, *SSA4* mRNA localizes to a nuclear dot in the *rna1-1* strain at 42°C, yet the poly(A) tail is only extended by 15–20 nt (data not shown). These observations also suggest that transcript sequestration per se does not cause extreme hyperadenylation. This leaves the precise relationship between transcript sequestration and adenylation effects uncertain. Indeed, we cannot observe an increase in *GAL1* poly(A) tail length after a shift to 37°C in the *rat7-1* background (data not shown). Although the fraction of long-tailed transcripts might be below the limit of detection by LM-PAT, this might indicate a dissociation between the dot and long-tail phenotypes for certain genes. Moreover, no hs-mRNA dots can be detected at 42°C in a yeast strain lacking both subunits of the PAN nuclease (ΔPAN2/3) despite a measurable poly(A) tail increase (data not shown; Brown and Sachs, 1998). This also suggests that PAN does not act at the site of transcription.

In several export mutants, the LM-PAT analysis shows a considerable amount of hs-mRNA with normal poly(A) tail lengths (Figure 5B). Furthermore, the nuclear mRNA export block in the ΔRIP1 strain at 42°C is incomplete (Vainberg et al., 2000), indicating that some transcripts below the detection limit of RNA-FISH must be released from the transcription site. These observations are consistent with results from the Parker laboratory showing that hyperadenylated transcripts are eventually chased into mRNAs with shorter tails (P. Hilleren and R. Parker, personal communication).

Perhaps the most compelling conclusion from this study is that cleaved and polyadenylated mRNA is released poorly from its transcription site when mRNA export is blocked. Our results strongly suggest that most if not all *SSA4* transcripts in the nuclear dot are hyperadenylated. First, oligo(dT)/RNase H-Northern assays show that all detectable *SSA4* transcripts are hyperadenylated in the ΔRIP1 strain at 42°C. Second, *SSA4* mRNA continues to increase in the nuclear dot after continued incubation (e.g., 60 min) at 42°C in a ΔRIP1 strain. It is unlikely that the 3′UTR probes are detecting such a prolonged accumulation of nascent transcripts. We therefore suggest that most if not all sequestered transcripts have undergone correct 3′-end cleavage and polyadenylation. This indicates that even in mammalian systems, mRNA-FISH signals at the site of transcription might be due to fully processed RNAs. Furthermore, these observations evoke the possibility that a defined release step exists before a processed mRNA can leave its transcription site. Such a step could reflect a checkpoint for correct mRNA 3′-end formation.

The fact that different mRNA export mutants all give

rise to similar mRNA-associated defects argues that the phenotypes are an indirect consequence of the temperature inactivation. Much needs to be learned about the exact roles of these proteins, but it is unlikely that they all exercise identical functions that impact directly on mRNA processing. Mex67p localizes to the nucleoplasm and the nuclear face of the NPC, whereas Rip1p, Nup159p, and Gle1p localize to the outer cytoplasmic part of the NPC (Segref et al., 1997; Rout et al., 2000). Although the localization data of Rip1p and Gle1p are somewhat controversial (Strahm et al., 1999), it is unlikely that all of these proteins share functions closely connected to 3′-end RNA processing and/or release of RNA from transcription sites. It is, therefore, possible that a block to nuclear export has indirect effects that influence events at the transcription site. For example, a nuclear export block could titrate a factor needed by newly synthesized transcripts for proper 3′-end processing and/or release. In such a scenario, nascent mRNAs require association with some factor/complex X prior to correct 3′-end formation and/or release of the transcript from the site of transcription. Under conditions where mRNA export is blocked, X would be sequestered on transcripts already in transit and exhausted from the pool present at transcription sites, resulting in local transcript accumulation. As hyperadenylation of *HSP104* and *SSA4* transcripts occurs extremely rapidly, this suggests that even very fast responses to restrictive temperature shifts can reflect indirect effects. Nonetheless, the uniform nature of the dot and hyperadenylation phenotypes suggests that they contribute to the mRNA export blocks. This is radically different from the canonical interpretation, which assigns the defects of many of these mRNA export mutants solely to interactions at or near the NPC.

Experimental Procedures

Yeast Strains, Primers, and Plasmids

S. cerevisiae strains and oligonucleotide primers used in this study are listed in supplemental Tables 1 and 2 (see www.molecule.org/cgi/content/full/7/4/887/DC1). The diploid ΔRIP1 strain was produced by mating of haploid ΔRIP1 strains of different mating types using standard techniques. Plasmids expressing low (RIP1-LO/pFS724) and high (RIP1-HI/pFS398) amounts of Rip1p as well as the plasmid expressing the C-terminal part of Rip1p (RIP1-0FG/pFS733) have been described previously (Stutz et al., 1997). pEC702, a 2 μ SSA4-expressing plasmid, has also been described (Boorstein and Craig, 1990).

Culture Growth, RNA Isolation, and In Vivo Protein Labeling

Yeast cultures were grown in YPD or appropriate dropout media at 25°C to an OD_{600} of 0.1. Dilute cultures were used in order to minimize stress conditions. Temperature shifts were performed by mixing a relevant volume of 25°C culture with an equal volume of 49°C media (for shift to 37°C) or 59°C media (for shift to 42°C), and shifted cultures were grown at the specified temperatures. Incubations were stopped by pouring cultures over crushed ice to ensure immediate cooling. Cells were collected by centrifugation, washed once with ice-cold H_2O, and stored at −80°C. Total RNA was extracted using either glass-bead lysis or hot acid phenol method (Ausubel et al., 1994). In vivo ^{35}S labeling of proteins was performed as described (Stutz et al., 1997).

Northern Blot and LM-PAT Analysis

Oligo(dT)/RNaseH Northern analysis were carried out as described (Salles et al., 1999). Twenty micrograms of total RNA was used for each reaction. To allow better resolution of individual bands, an oligonucleotide (thj261:5′-CACCTGCAGCTCCGT) antisense to a sequence in the 3′ end of the *SSA4* ORF was included in the RNaseH reaction. A oligo $(dT)_{18}$ was used for ablation of poly(A) tails. Samples were electrophoresed on 2% agarose/formaldehyde gels. Transfer to nitrocellulose membrane and probe hybridization was done as described (Ausubel et al., 1994), utilizing 5′-end radiolabeled kd199 and kd200 probes (see supplemental Table 2 at www.molecule.org/cgi/content/full/7/4/887/DC1) directed against the 3′UTR of *SSA4* RNA.

LM-PAT analysis was adapted from Salles et al. (1999). One microgram of total RNA and 20 ng phosphorylated oligo$(dT)_{18}$ was mixed in 7 μl H_2O and heated to 65°C for 10 min. The reaction was transferred immediately to 42°C and a mixture of 1 μl T4 DNA ligase (10 U/μl), 4 μl 5× AMV-RT buffer (250 mM Tris-HCl [pH 8.3], 40 mM MgCl2, 250 mM NaCl, 5 mM DTT), 1 μl Rnasin (40 U/μl), 2 μl 0.1 M DTT, 1 μl dNTP mix (10 mM each dNTP), 1 μl rATP (10 mM), and 3 μl H_2O was added, followed by a 30 min incubation. One microliter (200 ng/μl) of oligo(dT)-anchor (see supplemental Table 2 at www.molecule.org/cgi/content/full/7/4/887/DC1) was added, and samples were transferred to 16°C for 2 hr. After a 2 min incubation at 42°C, 1 μl of AMV-RT (10 U/μl) was added, and the incubation continued for 1 hr. AMV-RT was inactivated by a 20 min incubation at 65°C. One to three microliters of a 1:20 dilution of the cDNA sample was used for PCR as described previously (Salles et al., 1999). Conditions chosen for individual PCR reactions varied slightly depending on the primer used. A typical PCR reaction was the following: 94°C, 2 min; 2 cycles 94°C for 1 min, 50°C for 1 min, 72°C for 4 min; 24–26 cycles 94°C for 30 s, 50°C for 30 s, 72°C for 2 min; and 72°C for 7 min. To ensure generation of specific LM-PAT products, at least two different gene-specific primers were tested for each individual mRNA examined. For primer sequences, see supplemental Table 2 at www.molecule.org/cgi/content/full/7/4/887/DC1. Labeled PCR products were visualized by 5% urea polyacrylamide gel electrophoresis and autoradiography.

Bulk Poly(A) Length Determination

One to two micrograms total RNA were 3′-end labeled and digested with RNases as previously described (Minvielle-Sebastia et al., 1991). Reagents used were: 3′,5′-[5′-^{32}P]biphosphate (^{32}pCp; New England Nuclear), T4 RNA ligase (New England Biolabs), and RnaseA/T1 cocktail (Ambion). Radioactive samples were electrophoresed on 6%–8% polyacrylamide-urea gels, and products were visualized by autoradiography.

In Situ Hybridization Analysis

Briefly, cells were grown in YPD or appropriate dropout media at 25°C to an OD_{600} of 0.1. Cultures were temperature shifted by diluting with an equal volume of 49°C (for shifts to 37°C) or 59°C (for shift to 42°C) media. For Gal-induction experiments, cells were grown in medium containing 2% glycerol and 2% lactate as sole carbon sources. To induce gene expression, galactose was added to a total of 2%, and incubation was continued for 60 min. RNA-FISH analysis was carried out using Cy3 fluorochrome-conjugated oligonucletides as previously described (Long et al., 1997). *SSA4, HSP104*, and *GAL1* mRNAs were localized with a mixture of oligos as indicated in supplemental Table 2 (see www.molecule.org/cgi/content/full/7/4/887/DC1). Poly$(A)^+$ RNA was localized using a Cy3-labeled oligo$(dT)_{70}$ probe as described (Vainberg et al., 2000).

Acknowledgments

We thank Chuck Cole, Ed Hurt, Katja Strasser, and Francoise Stutz for yeast strains. Pascal Chartrand, Rob Singer, and Ken Dower are thanked for insights concerning RNA-FISH, and Irina Vainberg is thanked for intellectual input in the initial phase of the work. We are grateful to members of the Rosbash laboratory for discussions, to Patricia Hilleren and Roy Parker for communication of unpublished results, and to Francoise Stutz and Ken Dower for critical reading of the manuscript. Ed Dougherty is thanked for help with figures. T. H. J. was supported by stipends from the Carlsberg Foundation

and from the Howard Hughes Medical Institute. This work was supported by NIH grant GM 23549.

Received November 9, 2000; revised February 5, 2001.

References

Arts, G.J., Fornerod, M., and Mattaj, I.W. (1998). Identification of a nuclear export receptor for tRNA. Curr. Biol. *8*, 305–314.

Ausubel, F.M., Brent, R., Kingston, R.E., Moore, D.D., Seidman, J.G., Smith, J.A., and Struhl, K. (1994). Current Protocols in Molecular Biology (New York: Greene Publishing Associates).

Boorstein, W.R., and Craig, E.A. (1990). Structure and regulation of the SSA4 HSP70 gene of Saccharomyces cerevisiae. J. Biol. Chem. *265*, 18912–18921.

Brown, C.E., and Sachs, A.B. (1998). Poly(A) tail length control in Saccharomyces cerevisiae occurs by message-specific deadenylation. Mol. Cell. Biol. *18*, 6548–6559.

Custodio, N., Carmo-Fonseca, M., Geraghty, F., Pereira, H.S., Grosveld, F., and Antoniou, M. (1999). Inefficient processing impairs release of RNA from the site of transcription. EMBO J. *18*, 2855–2866.

Eckner, R., Ellmeier, W., and Birnstiel, M.L. (1991). Mature mRNA 3′end formation stimulates RNA export from the nucleus. EMBO J. *10*, 3513–3522.

Feldherr, C.M., Kallenbach, E., and Schultz, N. (1984). Movement of a karyophilic protein through the nuclear pores of oocytes. J. Cell Biol. *99*, 2216–2222.

Forrester, W., Stutz, F., Rosbash, M., and Wickens, M. (1992). Defects in mRNA 3′-end formation, transcription initiation, and mRNA transport associated with the yeast mutation *prp20*: possible coupling of mRNA processing and chromatin structure. Genes Dev. *6*, 1914–1926.

Gorlich, D., Dabrowski, M., Bischoff, F.R., Kutay, U., Bork, P., Hartmann, E., Prehn, S., and Izaurralde, E. (1997). A novel class of RanGTP binding proteins. J. Cell Biol. *138*, 65–80.

Gorsch, L.C., Dockendorff, T.C., and Cole, C.N. (1995). A conditional allele of the novel repeat-containing yeast nucleoporin *RAT7/NUP159* causes both rapid cessation of mRNA export and reversible clustering of nuclear pore complexes. J. Cell Biol. *129*, 939–955.

Huang, Y., and Carmichael, G.G. (1996). Role of polyadenylation in nucleocytoplasmic transport of mRNA. Mol. Cell. Biol. *16*, 1534–1542.

Hurt, E., Sträßer, K., Segref, A., Bailer, S., Schlaich, N., Presutti, C., Tollervey, D., and Jansen, R. (2000). Mex67p mediates nuclear export of a variety of RNA polymerase II transcripts. J. Biol. Chem. *275*, 8361–8368.

Izaurralde, E., Kutay, U., von Kobbe, C., Mattaj, I.W., and Gorlich, D. (1997). The asymmetric distribution of the constituents of the Ran system is essential for transport into and out of the nucleus. EMBO J. *16*, 6535–6547.

Katahira, J., Straßer, K., Podtelenikov, A., Mann, M., Jung, J.U., and Hurt, E. (1999). The Mex67p-mediated nuclear mRNA export pathway is conserved from yeast to human. EMBO J. *18*, 2593–2609.

Kutay, U., Lipowsky, G., Izaurralde, E., Bischoff, F.R., Schwarzmaier, P., Hartmann, E., and Gorlich, D. (1998). Identification of a tRNA-specific nuclear export receptor. Cell *1*, 359–369.

Long, R.M., Elliott, D.J., Stutz, F., Rosbash, M., and Singer, R.H. (1995). Spatial consequences of defective processing of specific yeast mRNAs revealed by fluorescence in situ hybridization. RNA *1*, 1071–1078.

Long, R.M., Singer, R.H., Meng, X., Gonzalez, I., Nasmyth, K., and Jansen, R. (1997). Mating type switching in yeast controlled by asymmetric localization of ASH1 mRNA. Science *277*, 383–387.

Mattaj, I.W., and Englmeier, L. (1998). Nucleocytoplasmic transport: the soluble phase. Annu. Rev. Biochem. *67*, 265–306.

Minvielle-Sebastia, L., Winsor, B., Bonneaud, N., and Lacroute, F. (1991). Mutations in the yeast RNA14 and RNA 15 genes result in an abnormal mRNA decay rate; sequence analysis reveals an RNA-binding domain in the RNA15 protein. Mol. Cell. Biol. *11*, 3075–3087.

Murphy, R., and Wente, S.R. (1996). An RNA-export mediator with an essential nuclear export signal. Nature *383*, 357–360.

Nakielny, S., and Dreyfuss, G. (1999). Transport of proteins and RNAs in and out of the nucleus. Cell *99*, 677–690.

Roth, F.P., Hughes, J.D., Estep, P.W., and Church, G.M. (1998). Finding DNA regulatory motifs within unaligned noncoding sequences clustered by whole-genome mRNA quantitation. Nat Biotechnol *16*, 939–945.

Rout, M.P., Aitchison, J.D., Suprapto, A., Hjertaas, K., Zhao, Y., and Chait, B.T. (2000). The yeast nuclear pore complex; composition, architecture, and transport mechanism. J. Cell Biol. *148*, 635–651.

Saavedra, C.A., Hammell, C.M., Heath, C.V., and Cole, C.N. (1997). Yeast heat shock mRNAs are exported through a distinct pathway defined by Rip1p. Genes Dev. *11*, 2845–2856.

Salles, F.J., Richards, W.G., and Strickland, S. (1999). Assaying the polyadenylation state of mRNAs. Methods *17*, 38–45.

Santos-Rosa, H., Moreno, H., Simos, G., Segref, A., Fahrenkrog, B., Pante, N., and Hurt, E. (1998). Nuclear mRNA export requires complex formation between Mex67p and Mtr2p at the nuclear pores. Mol. Cell. Biol. *18*, 6826–6838.

Sarkar, S., and Hopper, A.K. (1998). tRNA nuclear export in *Saccharomyces cerevisiae*: In situ hybridization analysis. Mol. Biol. Cell *9*, 3041–3055.

Schmitt, C., von Kobbe, C., Bachi, A., Pante, N., Rodrigues, J.P., Boscheron, C., Rigaut, G., Wilm, M., Seraphin, B., Carmo-Fonseca, M., and Izaurralde, E. (1999). Dbp5, a DEAD-box protein required for mRNA export, is recruited to the cytoplasmic fibrils of the nuclear pore complex via a conserved interaction with CAN/Nup159p. EMBO J. *18*, 4332–4347.

Segref, A., Sharma, K., Doye, V., Hellwig, A., Huber, J., Luhrmann, R., and Hurt, E. (1997). Mex67p, a novel factor for nuclear mRNA export, binds to both poly(A)$^+$ RNA and nuclear pores. EMBO J. *16*, 3256–3271.

Snay-Hodge, C.A., Colot, H.V., Goldstein, A.L., and Cole, C.N. (1998). Dbp5p/Rat8p is a yeast nuclear pore-associated DEAD-box protein essential for RNA export. EMBO J. *17*, 2663–2676.

Stoffler, D., Fahrenkrog, B., and Aebi, U. (1999). The nuclear pore complex: from molecular architecture to functional dynamic. Curr. Opin. Cell Biol. *11*, 391–401.

Strahm, Y., Fahrenkrog, B., Zenklusen, D., Rychner, E., Kantor, J., Rosbash, M., and Stutz, F. (1999). The RNA export factor Gle1p is located on the cytoplasmic fibrils of the NPC and physically interacts with the FG-nucleoporin Rip1p, the DEAD-box protein Rat8p/Dbp5p and a new protein Ymr255p. EMBO J. *18*, 5761–5777.

Straßer, K., Bassler, J., and Hurt, E. (2000). Binding of the Mex67p/Mtr2p heterodimer to FXFG, GLFG, and FG repeat nucleoporins is essential for nuclear mRNA export. J. Cell Biol. *150*, 695–706.

Stutz, F., and Rosbash, M. (1998). Nuclear RNA export. Genes Dev. *12*, 3303–3319.

Stutz, F., Kantor, J., Zhang, D., McCarthy, T., Neville, M., and Rosbash, M. (1997). The yeast nucleoporin Rip1p contributes to multiple export pathways with no essential role for its FG-repeat region. Genes Dev. *11*, 2857–2868.

Tseng, S.S., Weaver, P.L., Liu, Y., Hitomi, M., Tartakoff, A.M., and Chang, T.-H. (1998). Dbp5p, a cytosolic RNA helicase is required for poly (A)+ RNA export. EMBO J. *17*, 2651–2662.

Vainberg, I.E., Dower, K., and Rosbash, M. (2000). Nuclear export of heat shock and non-heat-shock mRNA occurs via similar pathways. Mol. Cell. Biol. *20*, 3996–4005.

Watkins, J.L., Murphy, R., Emtage, J.L., and Wente, S. (1998). The human homologue of Saccharomyces cerevisiae Gle1p is required for poly(A)+ RNA export. Proc.Natl.Acad.Sci.USA *95*, 6779–6784.

Wozniak, R.W., Rout, M.P., and Aitchison, J.D. (1998). Karyopherins and kissing cousins. Trends Cell Biol. *8*, 184–188.

Zhao, J., Hyman, L.E., and Moore, C. (1999). Formation of mRNA 3′ ends in eukaryotes: mechanism, regulation, and interrelationships with other steps in mRNA synthesis. Microbiol. Mol. Biol. Rev. *63*, 405–445.